Memorias del 2022 Congreso Nacional de Control Automático
12-14 de Octubre, 2022. Tuxtla Gutiérrez, México.

Bidirectional Buck-Boost converter as an Active Power Decoupling schema for Single-Phase Power Inverters

I. Yepez-Lopez * **V. Cárdenas** * **U. Cruz-Velazquez** *
H. Miranda * **J. Alcalá** **

* *Faculty of Engineering, Autonomous University of San Luis Potosi, San Luis Potosi, S.L.P. Av. Manuel Nava 8, 78290 (e-mail: iyepez@ieee.org, vcardena@uaslp.mx, cruzv.uriel@outlook.com, hmirandav@uaslp.mx).*
** *Faculty of Engineering, University of Colima, Colima, Manzanillo. Carretera Manzanillo-Barra de Navidad km 20.5, El Naranjo, 28860 (e-mail: janethalcala@ucol.mx).*

Abstract: The power ripple in the DC-link of photovoltaic and energy storage systems interconnected to the AC mains can drastically impact the lifespan of the photovoltaic panel and the system in general. This problem can be easily solved by using DC-link electrolytic capacitors as a passive decoupling method, however, this implies significant drawbacks such as increased volume and cost of the capacitor and a significant reduction in efficiency and reliability. This can be compensated by replacing electrolytic capacitors with active power decoupling methods based on power electronic converters. Thus, a Bidirectional Buck-Boost converter as an active power decoupling scheme is proposed. First, a power decoupling overview is addressed. Afterward, the operation of the Buck-Boost converter is detailed. Therefore, the control strategy is also explained. Finally, some simulations and preliminary experimental results to verify the integrated operation of the power converter are given.

Keywords: Active Power Decoupling, Power Ripple, Photovoltaic and Storage Systems, DC-DC and DC-AC Converters, Active Power Filters.

1. INTRODUCTION

Generally, a typical photovoltaic generation scheme interconnected to the AC mains is made up of two stages of power conversion: the DC/DC and DC/AC stages [Xu et al. (2018)]. The DC/DC converter meets the task of boosting the voltage on the DC link and supplying the Maximum Power Point (MPP) of the photovoltaic system [Sekiguchi and Shimizu (2019)]. The DC/AC converter (inverter) carries out the function of mapping the energy from the storage system and/or the photovoltaic system and supplying it to the AC mains. A sinusoidal current signal is generated at the inverter output that oscillates at a certain frequency (regularly 50Hz and 60Hz). An important aim of the power inverter is to decouple the energy in DC provided by the PV or the storage system from the power delivered to the AC grid. This separation is carried out through a process called *power decoupling*. Typically, this decoupling is based on a passive scheme and is undertaken by a DC capacitor called *link capacitor* [Michal (2016)], which filters the low and high-frequency AC components circulating across the DC side of the power inverter. This scheme has the advantage of being very simple because it is only necessary to use capacitors to perform the decoupling task. However, it also has numerous disadvantages such as the size and cost of this capacitor (regularly electrolytic), the reliability and lifespan, among others [Sun et al. (2016); Pereira et al. (2019)]. In applications with micro-inverters (250W) some proposals have been made for power decoupling to reduce the size of the link capacitor, thus being able to use film capacitors, which have higher efficiency, reliability, and a reduced volume. However, in higher power applications, it is necessary to integrate more suitable solutions. In this work, the development of a bidirectional Buck-Boost converter as an independent active power decoupling schema for photovoltaic and storage systems applications is proposed to reduce the link capacitor.

2. POWER DECOUPLING

An integrated photovoltaic generation scheme with AC mains coupling is usually the one shown in Fig. 1. As mentioned above, the DC/AC converter is responsible for mapping the energy from the DC link and turning it into AC for supplying energy to the AC grid. The output

of this converter is processed by a Low Pass Filter to remove high-frequency switching harmonics from the AC wave and supply a sinusoidal current at the determined frequency.

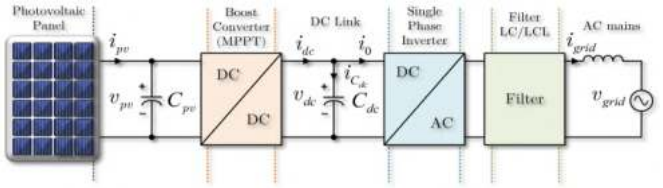

Fig. 1. Photovoltaic generation scheme with electrical grid coupling based on passive power decoupling.

The power on the DC link is given by the algebraic subtraction of the power at PV terminals minus the power supplied to the grid. The biggest drawback is that the power inverter needs to supply an instantaneous power that is oscillating, and when this happens, the power flowing in the DC link will automatically hold an oscillatory component at twice the fundamental frequency of the AC mains ($2\omega_0$). Consequently, the voltage on the DC link will also contain this oscillatory component and will be manifested as a voltage ripple [Aganza-Torres et al. (2014)]. This process arises analytically as follows:

Consider the photovoltaic generation system interconnected to the AC mains through a single-phase inverter represented by Fig. 1. Assuming a lossless operation, the power supplied by the DC link is given by Eq. 1.

$$P_{dc} = P_o = \frac{1}{T}\int_0^T p(t)\,dt = \frac{1}{T}\int_0^T v_{grid} i_{grid}\,dt \qquad (1)$$

If the voltage and current in the grid are given by $v_{grid} = V_p \cos(\omega_0 t)$ and $i_{grid} = I_p \cos(\omega_0 t - \phi)$, then the instantaneous power is given by $p(t) = v_{grid} i_{grid}$, that is:

$$p(t) = \frac{1}{2}[V_p I_p \cos(\phi) + V_p I_p \cos(2\omega_0 t - \phi)]. \qquad (2)$$

Whether the phase angle between the grid voltage and current (v_{grid} and i_{grid}) equals zero, the Eq. 2 can be rewritten as follows:

$$p(t) = P_o + P_o \cos(2\omega_0 t). \qquad (3)$$

It can be observed from Eq. 3 that the instantaneous output power is composed of two terms: the average power $P_o = V_p I_p/2$, which is constant, and a second term given by $P_o \cos(2\omega_o t)$ which oscillates at twice the frequency of the grid with an amplitude of the average power supplied at the output of the inverter. The oscillation is also present in the DC link voltage and at the PV terminals. This is critical especially for the PV since its efficiency is reduced and its lifespan is degraded. The simplest solution to this problem is to employ a passive decoupling scheme through energy storage elements (usually DC link capacitors). The sizing of the link capacitor can be determined by the following expression [Pereira et al. (2019)]:

$$C_{dc} \simeq \frac{P_{pv}}{\omega_0 V_{dc} \Delta V_{dc}}. \qquad (4)$$

As mentioned above, the problem lies mainly in the dimensioning of this capacitor. The proposed solution for this is to perform active power decoupling through power electronics converters replacing passive methods. Fig. 2 shows a structure that represents a basic example of active power decoupling interconnected to a DC/AC conversion scheme. In this case, there is a DC/DC converter that operates as an active power decoupling scheme; this converter is responsible for buffering the voltage ripple produced by the inverter when mapping the power from the DC link to the AC mains. The link capacitor is still preserved, however, it can be sized with a much lower value and can be replaced by film capacitors that have lower series resistances, making them ideal for higher power applications. In addition, as the volume of this capacitor is substantially reduced, the cost and efficiency are benefited in the same way.

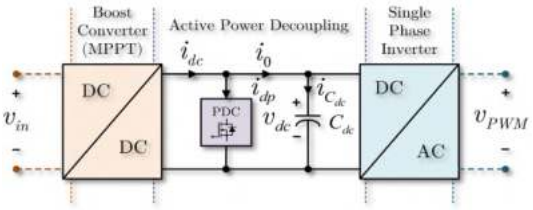

Fig. 2. Typical DC/AC conversion scheme based on active power decoupling.

2.1 Active Power Decoupling

Active power decoupling is a replacement for conventional passive decoupling schemes, but power electronics converters are used instead to carry out the power decoupling task.

Fig. 3 shows a single-phase inverter with an active power decoupling feature interconnected to the AC mains. It can be observed from the latter that the active power decoupling circuit can be represented by a current source that supplies a compensation current to the DC link to mitigate the power ripple that oscillates at ($2\omega_0$). The operation of this converter can be associated with what is well known as an *active filter* [Kafanas et al. (2016)]. Depending on the converter topology (series or parallel), it operates as a series or parallels active filter; the difference is that in the first case, it produces voltage drops to compensate for the ripple, while in parallel topologies the way to attenuate the ripple is through compensation currents [Sun et al. (2016)].

There exist numerous and different active power decoupling topologies, nevertheless, all this can be summarized in two simple categories: independent and dependent active power decoupling topologies. In independent topologies, there is a power converter as an active power decoupling scheme that operates fully apart from another power conversion stage. On the other hand, dependent

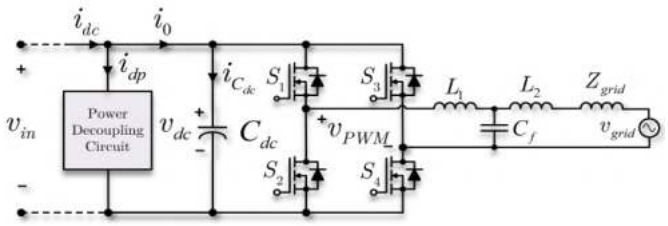

Fig. 3. Single phase inverter interconnected to the grid with active power decoupling feature.

topologies work together with another power conversion stage and may share power switches to perform two or more operation requirements [Sun et al. (2016)].

3. BIDIRECTIONAL BUCK-BOOST CONVERTER ANALYSIS AS AN ACTIVE POWER DECOUPLING SCHEME

In this work, the Bidirectional Buck-Boost converter is proposed as an active power decoupling scheme because it has numerous advantages of interest: it can operate individually in other conversion stages, then it has a modularity feature; the control system becomes simpler because the power switches meet only a unique task; and finally, as this topology has modularity feature, it can be easily replaced by a passive scheme to build comparisons scenarios and evaluate their performance.

The following considerations must be taken into account for the converter operation (Fig. 4) [Qiu et al. (2019); Kafanas et al. (2016)]:

(1) The decoupling capacitor C_z must bear large voltage ripple oscillations.
(2) The transfer inductor L operates in Discontinuous Current Mode (DCM).
(3) The stress voltage in power switches is $v_{dc} + v_{C_z}$.
(4) The stress current in power switches is given by i_{dc}/d, where d is the duty cycle.
(5) Both voltage and capacitance of the decoupling capacitor can be adjustable, but $v_{C_z} > 0$.

The function of this converter is to drive the current oscillatory harmonic of i_{dc} at $2\omega_0$, through the path of current i_{dp}; that is, they are equal, thus on the current i_0 demanded by the load, only the average value is manifested and the ripple energy is stored in the decoupling capacitor C_z. All this can be achieved by allowing a large voltage ripple on this decoupling capacitor; that is, the ripple energy is driven to be stored in C_z instead of C_{dc}, then only the high-frequency components are buffered by C_{dc}, and thus, this capacitance can be substantially reduced.

The bidirectional Buck-Boost converter has two power switches, S_1 and S_2, and can operate at first in a complementary way. The modulation scheme is very simple since it is possible to implement a constant PWM. The inductor L meets the task of transferring the power ripple energy from the DC link to the capacitor C_z. The converter

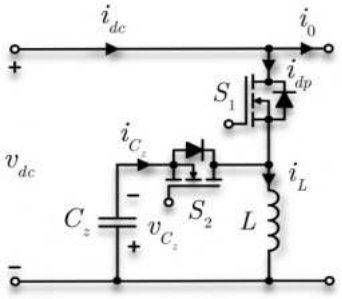

Fig. 4. Bidirectional Buck-Boost converter as a power decoupling scheme.

can operate in four different states [Nicieza (2017)]. The first takes place when switch S_1 is on and S_2 off. At this instant, current flows from the DC link towards the inductor which stores the energy, and the current tends to grow to a maximum value $i_{L_{max}}$. Once this maximum is reached, the second state takes place, where S_1 is off and the free-wheeling diode of S_2 is activated; in this state, the inductor transfers the energy to the capacitor and this is where the first cycle of the converter is completed. In the second cycle, the converter operates oppositely. In this case, the switch S_2 is on while S_1 is off and the decoupling capacitor C_z transfers the energy to the inductor L. At this point, switch S_2 is off, and the free-wheeling diode of the switch S_1 is activated, allowing the inductor current to circulate towards the DC link; this is where the four states of the power converter are completed.

Based on prior analysis, the following dimensioning equations can be determined [Qiu et al. (2019)]:

$$\left.\begin{aligned} D_{S_1} &= \sqrt{\frac{2i_{L_{avg}} f_s L}{v_{dc}}}, \quad L_1 \geq \frac{2v_{dc}v_{C_z}^2}{9I_{dc}f_s(v_{dc}+v_{C_z})^2}, \\ D_{S_2} &= \sqrt{\frac{2i_{L_{avg}} f_s L v_{dc}}{v_{C_z}^2}}, \quad L_2 \geq \frac{V_{dc}i_{L_{avg}}}{2f_s(I_p - i_{L_{max}})^2}, \\ & \qquad\qquad L > (L_1 \cup L_2). \end{aligned}\right\} \quad (5)$$

where D_{S_1} and D_{S_2} are the Duty Cycles for S_1 and S_2 respectively; L is the transfer inductor of the bidirectional Buck - Boost converter.

According to [Zhong et al. (2016)], the decoupling capacitor of the bidirectional Buck-Boost converter can be dimensioned by the initial DC link capacitor value and keeping in mind the rated power, the ratio of the average, and the ripple voltage on the DC link r_{dc} and the decoupling capacitor r_z. Thus, this capacitor can be determined as follows:

$$C_z \approx \frac{r_{dc}}{r_z}\left(\frac{V_{dc}}{V_{C_z}}\right)^2 C_{dc}. \quad (6)$$

4. CONTROL SYSTEM

A proper control system must be implemented for ensuring the performance of the power decoupling converter.

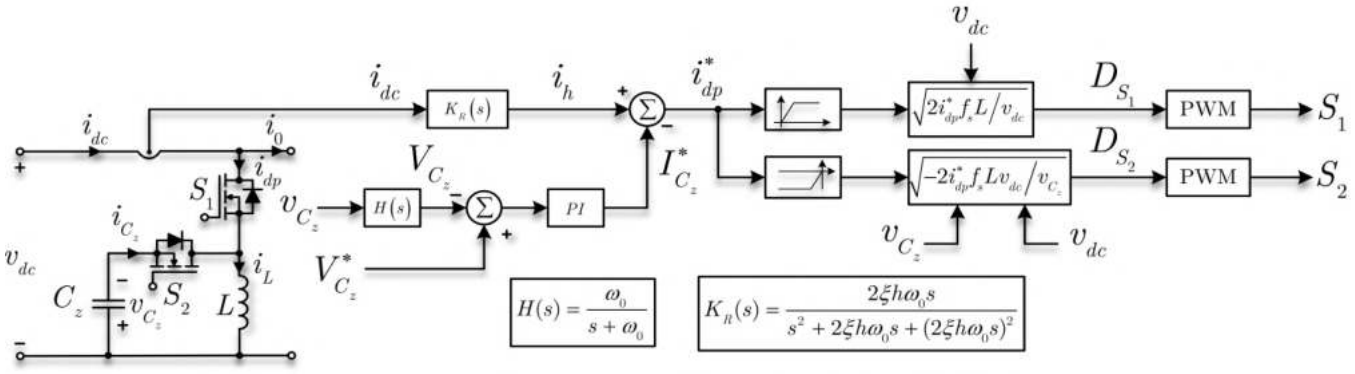

Fig. 5. Control strategy for the bidirectional Buck-Boost converter.

As mentioned in section 3, the bidirectional Buck-Boost converter aims to drive the low-frequency oscillatory current (i_h) at $2\omega_0$ through the power decoupling stage. All this results in the following control requirements:

- The oscillatory component of current i_{dc} must be equal to i_{dp}.
- The average voltage v_{C_z} must be regulated at a certain voltage level to keep the desired ripple voltage on the DC link.

According to [Cao et al. (2015)], there are essentially three well-known ways to perform the control strategy for the power decoupling converter. However, a simple and effective way to do so is by performing the control strategy shown in Fig. 5. It is necessary to measure the current i_{dc} that holds the oscillatory harmonic at $2\omega_0$. The measured current is subjected to a resonant filter $K_R(s)$, which provides the $2\omega_0$ component only, where $h = 2$ and $\omega_0 = 2\pi f$. Then, the average voltage of v_{C_z} can be obtained through a Low-Pass filter $H(s)$ (view Fig. 5).The average voltage V_{C_z} is compared with its reference and the error is subjected to a PI controller which provides the average capacitor current reference $I^*_{C_z}$; the subtraction of these two elements gives, as a result, the reference current i^*_{dp} which is used for calculating the duty cycle for each switch. Finally, a constant PWM is implemented to turn on and off the power switches. The structure of the PI controller can be represented by the Eq. 7

$$G_{PI}(s) = k_p\left(1 + \frac{1}{T_i s}\right). \tag{7}$$

5. SIMULATION RESULTS

In order to validate the operation of the active power decoupling converter, the simulation scheme shown in Fig. 6 was proposed. This scheme consists of a Voltage Source Converter (VSC) which operates as an active front rectifier that forms a DC link in which the power ripple is presented when it starts supplying power to the load. The decoupling schemes evaluated are a passive scheme (Fig. 6-(a)), composed of an electrolytic capacitor, and the active scheme based on the bidirectional Buck-Boost converter (Fig. 6-(b)). Simulation parameters are shown in Table 1.

Table 1. Simulation parameters.

Parameter	Value	Unit
Grid voltage v_{grid}	48	V_{rms}
DC link voltage v_{dc}	100	V_{prom}
Voltage ripple on the DC link Δv_{dc}	10	V
Rated power	200	W
Grid resistance R_{grid}	0.4	Ω
Grid inductance L_{grid}	5.5	mH
Load resistance R_{load}	50	Ω
Link capacitor (passive scheme) C_{cd}	640	μF
Decoupling capacitor (active scheme) C_z	100	μF
Transfer inductor L	620	μH
Switching frequency of VSC	10	kHz
Switching frequency of Buck-Boost converter	50	kHz

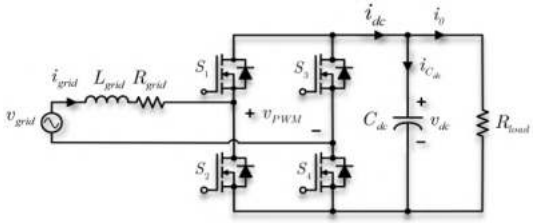

(a) VSC with passive power decoupling scheme.

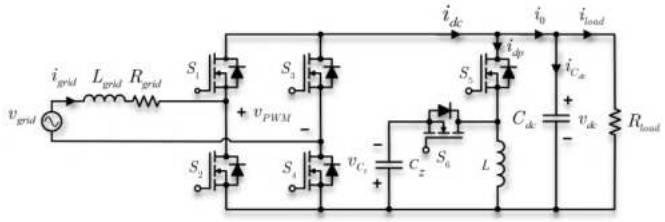

(b) VSC with active power decoupling scheme.

Fig. 6. Simulation scenarios.

Fig. 7-(a) shows the grid voltages and currents for both passive and active decoupling schemes where the power factor is unity. In both scenarios, it can be observed that the currents are the same because the power level in both schemas is the same. The first graph in Fig. 7-(b) shows that the DC link voltage is approximately $100V$ and has a ripple voltage of $10V$ for both passive and active decoupling schemas. The second graph shows the

voltage across the decoupling capacitor with a voltage ripple of approximately $35V$; it is important to highlight that the voltage across the switches is equal to the sum of the voltage level across the DC link and the decoupling capacitor. For this simulation, the circuit was dimensioned so that the voltage level in the switches did not exceed $300V$ at steady-state. The last graph in Fig. 7-(c) shows the inductor current in DCM, which has a half cycle positive and negative, reaching a maximum level no greater than $4A$ peak.

With the results obtained from these simulations, it can be theoretically concluded that the bidirectional Buck-Boost converter can properly operate as an active power decoupling converter and the design methods of the transfer inductor and decoupling capacitor are suitable for implementing an experimental prototype.

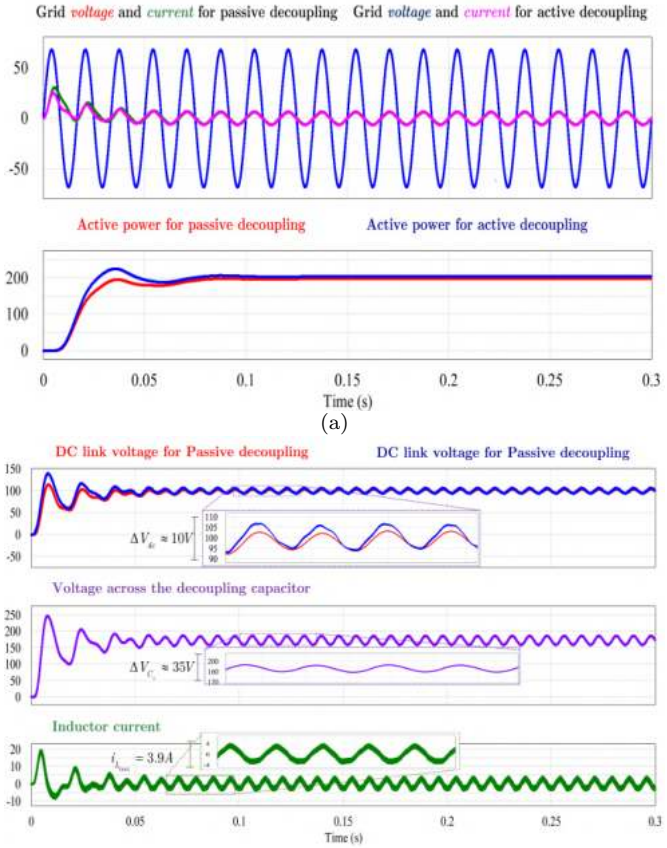

Fig. 7. Comparison between passive and active decoupling schemes.

6. EXPERIMENTAL RESULTS

The experimental scenario aims to validate in open-loop the design carried out for the foreseen power conditions and to perform a comparison between passive and active decoupling schemas. The final version of this work will include closed-loop results. It is important to remark that despite the experimental scenarios differ from the simulation scenarios, these are still legitimate and valid since independently of which scheme is used either the VSC as rectifier/inverter or the diode full-bridge rectifier, the power ripple at $2\omega_0$ is presented anyway and the magnitude of this power ripple relies on the supplied power and not on the scheme type. Furthermore, the change from the simulation to the experimental scenarios was performed for reasons of practicality and simplicity.

Fig. 8-(a) and 8-(b) show the first and second experimental scenarios respectively and Table 2 shows the parameters for these experiments; these two scenarios aim to validate the bidirectional Buck-Boost converter operating as an active power decoupling schema and to compare its performance with the passive power decoupling based on the electrolytic capacitor, both schemas coupled to a single-phase power inverter.

Table 2. Parameters for scenarios 1 and 2.

Parameter	Scenario 1	Scenario 2	Unit
Inverter output voltage	28.5	28.5	v_{rms}
DC link voltage	50	50	V_{prom}
Voltage ripple on the DC link	10	10	V
Rated power	50	50	W
Load resistance	16	16	Ω
DC link capacitor	1,100	100	μF
Decoupling capacitor	-	100	μF
Transfer inductor	-	620	μH
Inverter inductor	600	600	μH
Switching frequency of APDC	-	50	kHz
Switching frequency of VSC	20	20	kHz

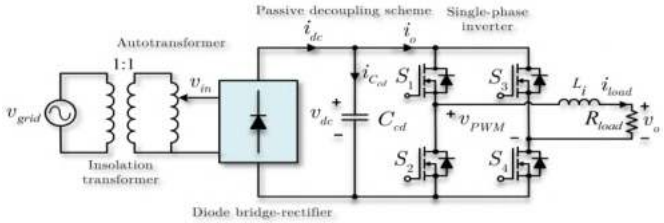

(a) First scenario.

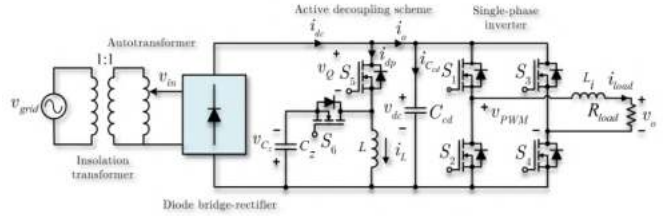

(b) Second scenario.

Fig. 8. Experimental scenarios.

From the results obtained in scenarios 1 and 2 (Fig. 9-(a) and 9-(b) respectively), it can be observed that both passive and active schemas are working properly and accomplishing the task of power decoupling since the voltage ripple is buffered. It is important to remark that the duty cycle (D) of the bidirectional Buck-Boost converter is set to 80% for a safety margin, then the voltage ripple can be further reduced, and thus, the harmonic distortion for the active decoupling schema can equal that of the passive schema or even less. Channels 1

and 3 show the output voltage and current of the inverter. Channel 2 displays the DC link voltage and finally the Math Channel illustrates the active power supplied by the inverter.

7. CONCLUSION

In the wake of the results obtained in this work, it can be concluded that the bidirectional Buck-Boost converter can properly operate as an active power decoupling schema. This topology could certainly work hand-in-hand with the full-bridge power inverter, however, it has the versatility to be integrated into different power conversion applications. Despite this, it needs two power switches for performing the decoupling task and this implies that power losses will increase. During the experimental tests, it could be noticed that parasitic capacitance and inductance in the PCB were critical because they limited drastically the rated power at which the converter could safely operate due to the voltage and current overshoots presented on the power switches. Despite this, from the analysis and the results obtained, it can be concluded that for the converter design carried out in this work, the total required capacitance could be reduced up to 5.5 times the initial DC link capacitance which allows suitably the use of film capacitors instead of electrolytic. In future work, a deeper comparison remains to be performed between the passive and the active schemas in which can be considered issues such as power losses, efficiency and real cost balance.

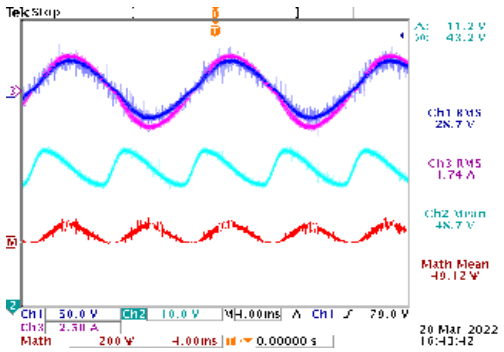

(a) First scenario.

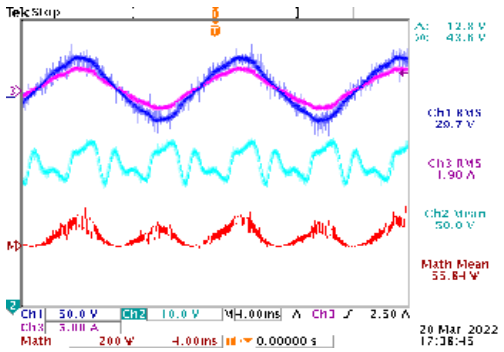

(b) Second scenario.

Fig. 9. Experimental results. *Ch1:* Inverter output voltage - v_o. *Ch2:* DC link voltage - v_{dc}. *Ch3:* Inverter output current - i_{load}. *MathCh:* Active power - P_o.

REFERENCES

Aganza-Torres, A., Cárdenas, V., Miranda-Vidales, H., and Alcalá, J. (2014). Decoupling capacitor minimization in hf-link single-phase cycloconverter based microinverter. *Solar Energy*, 105, 590–602. doi: https://doi.org/10.1016/j.solener.2014.04.013.

Cao, X., Zhong, Q.C., and Ming, W.L. (2015). Ripple eliminator to smooth dc-bus voltage and reduce the total capacitance required. *IEEE Transactions on Industrial Electronics*, 62(4), 2224–2235. doi: 10.1109/TIE.2014.2353016.

Kafanas, G., Jeffrey, M.R., and Yuan, X. (2016). Variable structure control for active power decoupling topologies. In *8th IET International Conference on Power Electronics, Machines and Drives (PEMD 2016)*, 1–6. doi:10.1049/cp.2016.0170.

Michal, V. (2016). Switched-mode active decoupling capacitor allowing volume reduction of the high-voltage dc filters. *IEEE Transactions on Power Electronics*, 31(9), 6104–6111. doi:10.1109/TPEL.2015.2500920.

Nicieza, L. (2017). Dc-link cancellation in single phase converters.

Pereira, T.A., Martins, D.C., and Coelho, R.F. (2019). Active-capacitor for power decoupling in single-phase grid-connected converters. In *2019 IEEE 15th Brazilian Power Electronics Conference and 5th IEEE Southern Power Electronics Conference (COBEP/SPEC)*, 1–6. doi:10.1109/COBEP/SPEC44138.2019.9065863.

Qiu, M., Wang, P., Bi, H., and Wang, Z. (2019). Active power decoupling design of a single-phase ac–dc converter. 18.

Sekiguchi, T. and Shimizu, T. (2019). Study on single-phase photovoltaic power generation system with power decoupling and generation control functions. In *2019 10th International Conference on Power Electronics and ECCE Asia (ICPE 2019 - ECCE Asia)*, 1945–1951. doi:10.23919/ICPE2019-ECCEAsia42246.2019.8797080.

Sun, Y., Liu, Y., Su, M., Xiong, W., and Yang, J. (2016). Review of active power decoupling topologies in single-phase systems. *IEEE Transactions on Power Electronics*, 31(7), 4778–4794. doi: 10.1109/TPEL.2015.2477882.

Xu, S., Mao, M., Shao, R., and Chang, L. (2018). Voltage-reference active power decoupling based on boost converter for single-phase bridge inverter. In *2018 International Power Electronics Conference (IPEC-Niigata 2018 -ECCE Asia)*, 1793–1798. doi: 10.23919/IPEC.2018.8507875.

Zhong, Q.C., Ming, W.L., Cao, X., and Krstic, M. (2016). Control of ripple eliminators to improve the power quality of dc systems and reduce the usage of electrolytic capacitors. *IEEE Access*, 4, 2177–2187. doi: 10.1109/ACCESS.2016.2561269.